Slow synaptic dynamics in a network: From exponential to power-law forgetting

J. M. Luck[1,*] and A. Mehta[2,†]

[1]*Institut de Physique Théorique, URA 2306 of CNRS, CEA Saclay, 91191 Gif-sur-Yvette Cedex, France*

[2]*S. N. Bose National Centre for Basic Sciences, Block JD, Sector 3, Salt Lake, Calcutta 700098, India*

(Received 18 July 2014; published 30 September 2014)

We investigate a mean-field model of interacting synapses on a directed neural network. Our interest lies in the slow adaptive dynamics of synapses, which are driven by the fast dynamics of the neurons they connect. Cooperation is modeled from the usual Hebbian perspective, while competition is modeled by an original polarity-driven rule. The emergence of a critical manifold culminating in a tricritical point is crucially dependent on the presence of synaptic competition. This leads to a universal $1/t$ power-law relaxation of the mean synaptic strength along the critical manifold and an equally universal $1/\sqrt{t}$ relaxation at the tricritical point, to be contrasted with the exponential relaxation that is otherwise generic. In turn, this leads to the natural emergence of long- and short-term memory from different parts of parameter space in a synaptic network, which is the most original and important result of our present investigations.

DOI: 10.1103/PhysRevE.90.032709 PACS number(s): 87.19.lv, 87.18.Sn, 87.10.Mn, 05.40.−a

I. INTRODUCTION

Memory and its mechanisms have always attracted a great deal of interest [1]. It is well known that memory is not a monolithic construct, and that memory subsystems corresponding to episodic, semantic, or working memory exist [2]. We focus here on explicit memory, which is the memory for events and facts.

In general, memories are acquired by the process of learning, which is a complicated phenomenon related to neural activities, brain network structure, and synaptic plasticity [3]. However, neuroscientists [4,5] typically focus on the latter, so that increasingly sophisticated models of synaptic plasticity have emerged over the years [6–8]. Much of this work has been done by adapting methods from statistical physics. Such modeling, while it may not include details of specificities involving chemical and biological processes in the brain, can outline possible mechanisms that take place in simplified structures. For example, the study of neural networks [6–8], while it greatly simplifies biological structures in order to make them tractable, has still been able to make an impact on the parent field. In particular, neural networks such as the Hopfield model [9,10] have been extensively investigated via methods borrowed from the statistical physics of disordered and complex systems [11–14]. In these models, memories are stored as patterns of neural activities, which correspond both to low-energy states and to attractors of the stochastic dynamics of the model. An essential property of these models as well as real neural networks is that their capacity is finite. Forgetting is therefore an important aspect of continued learning [3,15–20].

More recently, there has been a great deal of work on the fast dynamics of neurons in neural networks. Typically, models of integrate-and-fire neurons on networks have been studied, and their different dynamical regimes explored [21]. The discovery of neural avalanches in the brain [22] was followed by several dynamical models of neural networks [23,24], where the statistics of avalanches were investigated [25–30] in the context of theories of self-organized criticality [31]. A review of such approaches can be found in Ref. [32].

Here, by contrast, we study the slow dynamics of adaptive synapses in neural networks. This is done with the objective of exploring the phenomena of learning and forgetting, to both of which the evolution of synaptic plasticity is strongly linked [3].

We usually tend to remember information only for relatively short durations: such finite time scales, corresponding to short-term memory, are readily modeled by a process of exponential forgetting. However, there are some things we remember for as long as we live, which form part of our long-term memories: this scenario corresponds to power-law forgetting [33–35], with its attendant absence of time scales. Typically, models that manifest the latter have made use of specially designed synapses with hidden internal states [36–38]. The aim of this paper is to provide a holistic framework for the modeling of synaptic networks that are capable of storing both long- and short-term memories, without recourse to specialized architectures. In our model, these emerge naturally in different parameter regimes, as a direct consequence of the collective dynamics of synaptic cooperation and competition. Our model thus provides a clear modeling alternative to the cascade process of Fusi and collaborators [36], which have so far occupied center stage in the field: while their model invokes specialized synaptic architectures to get long-term memory, ours does not.

In general, neural processes are assumed to be subject to local rules that govern the way in which synapses are updated [3,39]; Hebb's rule is an important example, which says that "neurons that fire together, wire together" [40]. The outcome of many such processes results in functional change, which drives behavior, in much the same way as in agent-based modeling, when local interactions among agents may give rise to emergent phenomena on a macroscopic scale [41]. In such approaches [42], the underlying idea is that the strategy of a given agent is to a large extent determined by what the others are doing, through considerations of the relative payoffs obtainable in each case. This formalism was extended

*jean-marc.luck@cea.fr

†anita@bose.res.in

 ©2014 American Physical Society

to neural networks in a simple-minded way in Refs. [43,44], where synapses adapted via competing interactions involving the activity patterns of interconnected neurons.

This paper puts that earlier work on a more complete footing, in particular by extending the types of synaptic interactions. It is known that both competition and cooperation play important roles in synaptic plasticity [45]; cooperation has traditionally been modeled by Hebb's rule, but this alone can lead to the unlimited growth of synaptic strength, which is unphysical. Competition is thus a necessary mechanism to regulate such growth [4,46]: while regarded as an essential ingredient by neuroscientists, its inclusion in theoretical models is rare [5]. An example of competition in the fast dynamical regime of firing neurons can be found in Ref. [47], where synaptic updates occur depending on the latency of spike trains. Our modeling of competition [43] is, however, formulated in the opposite dynamical regime of slow synaptic dynamics. Finally, we also include a representation of the spontaneous relaxation of synapses. This mechanism is an important one in the context of finite storage capacities, when space is created via the spontaneous decay of old memories. This is sometimes referred to as the palimpsest effect [15,16].

At the most microscopic level, individual neurons fire at rates that exhibit a whole spectrum of biological noise [6–8]. Here we choose a level of description where neurons may be either active or inactive, according to their mean firing rates. The response of neurons is considered as stochastic and instantaneous with respect to the much slower dynamics of the synapses we consider. As a result of this temporal coarse graining, the overall effect of the microscopic noise can be represented by spontaneous relaxation rates from one type of synaptic strength to the other. Next, cooperation between synapses is incorporated via the usual Hebbian viewpoint. Our modeling of the competitive interaction by polarity-driven interactions is the most original as well as the most crucial part of our formalism: synapses are converted to the type most responsible for neural activity in their neighborhood [43,44].

Our choice of basis is that of a fully connected network, where all neurons are connected to one another by directed synapses [6,8]. Section II contains a detailed description of the model. In Sec. III, we characterize the various types of mean-field dynamics (generic, critical, tricritical) displayed by our model. In Sec. IV, we explore the dependence of our phase diagram on parameters, with particular reference to the behavior of relaxation times. In Sec. V, we address issues related to learning and forgetting, and show that our model contains a rich spectrum of time scales. Finally, in Sec. VI, we discuss our findings.

II. MODEL

We model a network of neurons connected by directed synapses. We first describe the geometry of our network and then explain the nature of its dynamics.

A. Geometry

We consider a fully connected network, whose bonds are directed (see Fig. 1) by randomly attributing an orientation to every bond of the complete graph on N nodes. With this geometry, mean-field theory is expected to apply in the thermodynamic limit of an infinitely large network [6].

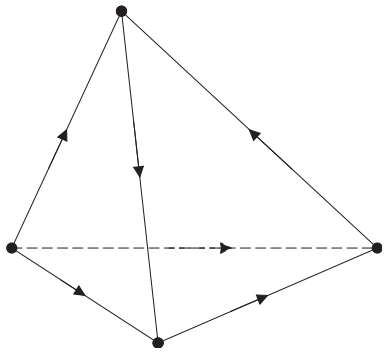

FIG. 1. An instance of the directed fully connected network with four nodes.

We mention in passing that our assumption of a fully connected network in our analysis is only for technical simplicity. In fact, mean-field dynamics are also expected to apply to sparse networks, provided that the degree (number of neighbors) of its nodes grows to infinity with the system size N. Realistic neural networks, while sparse, indeed show such growth [48,49], so that it is valid to do a mean-field analysis of their dynamics. It turns out that for such networks, the degree grows linearly with system size; it is of the form pN where p is of the order of 10–15 % .

Neurons live on the nodes of the network, labeled $i = 1, \ldots, N$. The activity state of neuron i at time t is described by a binary activity variable:

$$\nu_i(t) = \begin{cases} +1 & \text{if } i \text{ is active at time } t, \\ -1 & \text{if } i \text{ is inactive at time } t. \end{cases} \tag{1}$$

Active neurons are those whose instantaneous firing rate exceeds some unspecified threshold.

The network is equipped with oriented bonds as follows. For each pair of different nodes i and j, we attribute a random orientation to the bond joining i and j, i.e., we put with probability $\frac{1}{2}$ either a directed bond (ij) from i to j, or a directed bond (ji) from j to i, but never both. The total number of oriented bonds is therefore $\frac{1}{2}N(N-1)$. Synapses live on the directed bonds (ij) so defined. The strength $\sigma_{ij}(t)$ of synapse (ij) at time t is also described by a binary variable:

$$\sigma_{ij}(t) = \begin{cases} +1 & \text{if } (ij) \text{ is strong at time } t, \\ -1 & \text{if } (ij) \text{ is weak at time } t. \end{cases} \tag{2}$$

Strong synapses are those whose strength exceeds some unspecified threshold.

B. Neuronal dynamics

Neurons have an instantaneous stochastic response to their environment. The activity of neuron i at time t reads

$$\nu_i(t) = \begin{cases} +1 & \text{with probability } F[h_i(t)], \\ -1 & \text{with probability } 1 - F[h_i(t)], \end{cases} \tag{3}$$

where $F(h)$ is a sigmoidal response function of the input field $h_i(t)$, increasing from $F(-\infty) = 0$ to $F(+\infty) = 1$. The input

field acting on neuron i,

$$h_i(t) = \frac{1}{N} \sum_{j \in \partial(i)} [a + b\sigma_{ji}(t)]\nu_j(t), \tag{4}$$

is a weighted sum of the instantaneous activities $\nu_j(t)$ of the neurons j, which influence i. Here, $\partial(i)$ denotes the subset of nodes j, which transmit information to i via directed synapses (ji). Strong synapses ($\sigma_{ji} = 1$) enter the above sum with a synaptic weight $a + b$, while weak ones ($\sigma_{ji} = -1$) have a synaptic weight $a - b$. We assume a and b are constant all over the network.

All synapses are therefore excitatory for $b > 0$, and inhibitory for $b < 0$. The kind of collective behavior discussed here, either along the critical manifold of at its tricritical endpoint, is therefore different in nature from the chaotic dynamical features, which have been emphasized in balanced networks [50–52], where excitatory and inhibitory effects balance each other on average.

In the following, we consider a spatially homogeneous situation in the thermodynamic limit of an infinitely large network. In this limit, for every node i, the numbers of incoming bonds (ji) and outgoing bonds (ik) are both equal to $\frac{1}{2}N$, up to negligible fluctuations. Moreover, we focus on the slow plasticity dynamics of the synaptic strengths. The characteristic time scale of this dynamics is much larger than the microscopic time scale of neural activity. Within this framework, it will be sufficient to consider the mean neural activity

$$A(t) = \frac{1}{N} \sum_i \nu_i(t) \tag{5}$$

and the mean synaptic strength

$$J(t) = \frac{2}{N(N-1)} \sum_{(ij)} \sigma_{ij}(t). \tag{6}$$

These key dynamical quantities entirely characterise the global aspects of the slow synaptic dynamics. They are related by a constitutive equation of the form

$$A(t) = g[J(t)], \tag{7}$$

which is local in time: the mean neural activity $A(t)$ only depends on the mean synaptic strength $J(t)$ at the same time t. The form of the function $g(J)$ can, at least in principle, be derived by appropriately averaging the microscopic equations (3) and (4), both spatially over the network and temporally over an integration time Δt, which would be large with respect to the time interval between two spikes, say, and very small with respect to the characteristic time scale of plasticity dynamics.

In this work, we prefer to employ a more phenomenological route. Remember that all the synapses of the network are excitatory for $b > 0$, and inhibitory for $b < 0$. Consider for a while the special situation where there are as many strong as weak synapses. In this case the mean synaptic strength defined in (6) vanishes ($J = 0$). We make the simplifying assumption that there are also as many active as inactive neurons on average in this situation, so that $A = 0$. Then, linearising the constitutive equation (7) around this symmetric situation, we readily obtain the linear response formula

$$g(J) = \varepsilon J, \tag{8}$$

which will be used throughout this work. The slope ε of the response function is one of the key parameters of the model. It is clearly proportional to b, and positive in the excitatory case ($b > 0$), so that $g(J)$ is an increasing function of J. In the inhibitory case ($b < 0$), ε is negative, so that $g(J)$ is a decreasing function of J. Finally, it has to obey $|\varepsilon| < 1$.

C. Synaptic plasticity dynamics

Synaptic strengths evolve very slowly in time, compared to the fast time scales of neuron firing rates. It is thus natural to model synaptic dynamics as a stochastic process in continuous time [53], defined in terms of effective jump rates between the two states, strong or weak, of the synaptic strength. Our model includes three plasticity mechanisms, which drive synaptic evolution:

1. Spontaneous relaxation mechanism

Synapses may spontaneously change their state from weak to strong (potentiation) or strong to weak (depression). This spontaneous relaxation mechanism translates into

$$\begin{aligned} \sigma_{ij} = -1 \to +1 \quad &\text{with rate } \Omega, \\ \sigma_{ij} = +1 \to -1 \quad &\text{with rate } \omega. \end{aligned} \tag{9}$$

Signal processing, in this context, examines the effect of deterministic external signals which are superposed on these spontaneous relaxation rates [see (42)].

2. Hebbian mechanism

When two neurons are in the same state of activity (inactivity), the synapse which connects them strengthens; when one of the neurons is active and the other is not, the interconnecting synapse weakens. This is the well-known Hebbian mechanism [40], which we implement with rate α. In the thermodynamic limit of the directed fully connected network, the probability to have $\nu_i = \pm 1$ at any given time is $\frac{1}{2}(1 \pm A) = \frac{1}{2}[1 \pm g(J)]$. The probabilities q_+ (q_-) to have $\nu_i = \nu_j$ ($\nu_i \neq \nu_j$) are:

$$q_\pm = \tfrac{1}{2}[1 \pm g(J)^2]. \tag{10}$$

We thus have

$$\begin{aligned} \sigma_{ij} = -1 \to +1 \quad &\text{with rate } \alpha q_+, \\ \sigma_{ij} = +1 \to -1 \quad &\text{with rate } \alpha q_-. \end{aligned} \tag{11}$$

3. Polarity-driven mechanism

This is a mechanism to introduce synaptic competition, introduced for the first time in Ref. [43], which converts a given synapse to the type of its most successful neighbors. Thus: if a synapse (ij) connects two neurons with different activities at any given time, it will adapt its strength to that of a randomly selected synapse connected to the active neuron. If we have $\nu_i = +1$ and $\nu_j = -1$, the active neuron i is presynaptic, and the selected synapse may be either outgoing (ik) from neuron i, or incoming (ki) to neuron i. If we have $\nu_i = -1$ and $\nu_j = +1$, the active neuron j is postsynaptic, and the selected synapse may be either outgoing (jk) from neuron j, or incoming (kj)

to neuron j. If the selected synapse is strong, the update $\sigma_{ij} = -1 \to +1$ takes place with rate β; if it is weak, the update $\sigma_{ij} = +1 \to -1$ takes place with rate γ. The rates β and γ are assumed to be identical in all four cases.

All in all, the polarity-driven mechanism also translates into a simple form in the thermodynamic limit of the directed fully connected network:

$$\begin{aligned} \sigma_{ij} = -1 \to +1 \quad &\text{with rate } \tfrac{1}{2}\beta(1+J)q_-, \\ \sigma_{ij} = +1 \to -1 \quad &\text{with rate } \tfrac{1}{2}\gamma(1-J)q_-. \end{aligned} \tag{12}$$

III. MEAN-FIELD DYNAMICS

Here we begin our investigation of the slow collective dynamics of the synaptic activity in the network: importantly, we restrict ourselves to its global features, rather than looking at patterns of spatially varying synaptic strengths.

For a spatially homogeneous situation in the thermodynamic limit, the mean synaptic strength $J(t)$ obeys a nonlinear dynamical mean-field equation of the form

$$\frac{dJ}{dt} = P(J). \tag{13}$$

The explicit form of the rate function $P(J)$ is obtained by summing the contributions of the three plasticity mechanism mentioned above:

$$P(J) = P_1(J) + P_2(J) + P_3(J), \tag{14}$$

with [see (9), (11), (12)]

$$\begin{aligned} P_1(J) &= \Omega(1-J) - \omega(1+J), \\ P_2(J) &= \alpha\left(g(J)^2 - J\right) \\ &= -\alpha J(1-\varepsilon^2 J), \\ P_3(J) &= -\delta(1-J^2)[1-g(J)^2] \\ &= -\delta(1-J^2)(1-\varepsilon^2 J^2), \end{aligned} \tag{15}$$

where

$$\delta = \tfrac{1}{4}(\gamma - \beta). \tag{16}$$

In the most general situation, the model has five parameters: the slope ε of the linear response equation (8) and the four rates Ω, ω, α, and δ involved in the three plasticity mechanisms. The resulting rate function is a polynomial of degree 4:

$$P(J) = p_4 J^4 + p_2 J^2 - (\Omega + \omega + \alpha)J + \Omega - \omega - \delta, \tag{17}$$

with

$$p_4 = -\delta\varepsilon^2, \quad p_2 = (\alpha + \delta)\varepsilon^2 + \delta. \tag{18}$$

The linear rate function $P_1(J)$ corresponds to the spontaneous mechanism; the Hebbian mechanism leads to the quadratic nonlinearity of $P_2(J)$, while the polarity-driven competitive mechanism results in the quartic nonlinearity of $P_3(J)$.

The parameter ε only enters (15) and (18) through its square ε^2. The model therefore exhibits an exact symmetry between the excitatory ($\varepsilon > 0$) and the inhibitory ($\varepsilon < 0$) cases. This is to be expected, as none of the plasticity mechanisms distinguishes between them. More generally, the model is invariant if the constitutive function $g(J)$ is changed into its opposite.

A. Generic dynamics

The dynamics leave the mean synaptic strength confined to the physical interval $-1 \leqslant J(t) \leqslant 1$. We have indeed $P(-1) = 2\Omega + \alpha(1+\varepsilon^2) > 0$ and $P(1) = -2\omega - \alpha(1-\varepsilon^2) < 0$. The rate function $P(J)$ has therefore an odd number of zeros in this interval, i.e., either one or three, with appropriate multiplicities in critical regimes. These zeros correspond to fixed points of the dynamics. As a consequence, the model exhibits two generic dynamical regimes, as shown in Fig. 2.

In regime I (see Fig. 2, top), there is a single attractive (stable) fixed point at J_0. The mean synaptic strength $J(t)$ therefore converges exponentially fast to this unique fixed point, irrespective of its initial value, according to

$$J(t) - J_0 \sim \mathrm{e}^{-t/\tau_0}. \tag{19}$$

The corresponding relaxation time reads

$$\tau_0 = -\frac{1}{P'(J_0)}. \tag{20}$$

In the limiting situation where there is only spontaneous relaxation, so that $P(J) = P_1(J)$, we have

$$J_0 = \frac{\Omega - \omega}{\Omega + \omega}, \quad \tau_0 = \frac{1}{\Omega + \omega}. \tag{21}$$

In regime II (see Fig. 2, bottom), there are two attractive (stable) fixed points at J_1 and J_2, and an intermediate repulsive (unstable) one at J_3. The mean synaptic strength $J(t)$ converges exponentially fast to either of the attractive fixed points, depending on its initial value, namely to J_1 if $-1 < J(0) < J_3$ and to J_2 if $J_3 < J(0) < 1$. The corresponding relaxation times read

$$\tau_1 = -\frac{1}{P'(J_1)}, \quad \tau_2 = -\frac{1}{P'(J_2)}. \tag{22}$$

In other words, regime II allows for the coexistence of two separate fixed points, leading to network configurations which are composed of largely strong/weak synapses. The quartic

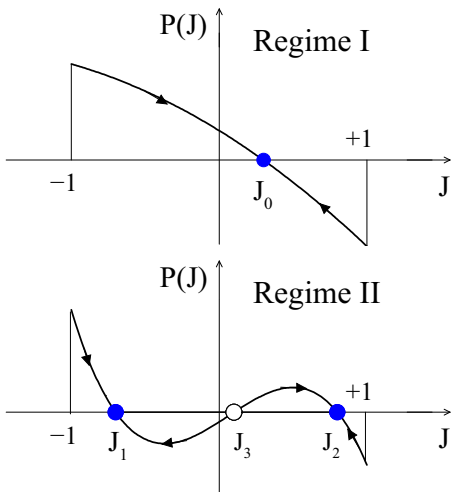

FIG. 2. (Color online) The two possible generic dynamical regimes. Top: Regime I (one single attractive fixed point, J_0). Bottom: Regime II (two attractive fixed points, J_1 and J_2, and an intermediate repulsive one, J_3).

nonlinearity corresponding to the polarity-driven plasticity mechanism needs to be sufficiently strong for the model to exhibit this coexistence (see Sec. IV).

B. Critical dynamics

When two of the three fixed points merge at some J_c, the dynamical system (13) exhibits a saddle-node bifurcation [54]. In physical terms, the dynamics become critical. We have then

$$P(J_c) = P'(J_c) = 0, \tag{23}$$

so that the critical synaptic strength J_c is a double zero of the rate function $P(J)$ (see Fig. 3). There is a left critical case, where $J_1 = J_3 = J_c^{(\mathrm{L})}$, while J_2 remains noncritical, and a right one, where $J_2 = J_3 = J_c^{(\mathrm{R})}$, while J_1 remains noncritical. The critical synaptic strength J_c in both cases will be shown to obey $J_c > \frac{1}{3}$ [see (36)]. We thus conclude that the critical point is always strengthening, as J_c is always larger than the natural initial value $J(0) = 0$, corresponding to a random mixture of strong and weak synapses in equal proportions.

The mean synaptic strength exhibits a universal relaxation to its critical value, of the form

$$J(t) - J_c \approx \frac{A_c}{t}. \tag{24}$$

The corresponding amplitude reads

$$A_c = -\frac{2}{P''(J_c)} = \frac{1}{6\delta\varepsilon^2\left(J_c^2 - J_T^2\right)}. \tag{25}$$

The expression (30) for J_T^2 as a function of ε, α, and δ has been used to derive the equality on the extreme right. The $1/t$ relaxation law (24) holds whenever the initial value $J(0)$, is on the attractive side of the critical point, i.e., $-1 < J(0) < J_c^{(\mathrm{L})}$ in the left critical case (where $J_c^{(\mathrm{L})} < J_T$ and so $A_c^{(\mathrm{L})} < 0$), or $J_c^{(\mathrm{R})} < J(0) < 1$ in the right critical one (where $J_c^{(\mathrm{R})} > J_T$ and so $A_c^{(\mathrm{R})} > 0$). In the opposite regimes [$J_c^{(\mathrm{L})} < J(0) < 1$ in the left critical case or $-1 < J(0) < J_c^{(\mathrm{R})}$ in the right critical case], one finds exponential relaxation to J_2 and J_1 respectively.

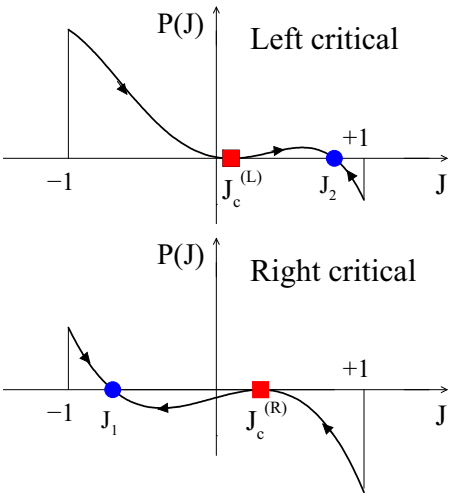

FIG. 3. (Color online) The two possible kinds of critical dynamical behavior. Top: left critical case ($J_1 = J_3 = J_c^{(\mathrm{L})}$). Bottom: right critical case ($J_2 = J_3 = J_c^{(\mathrm{R})}$).

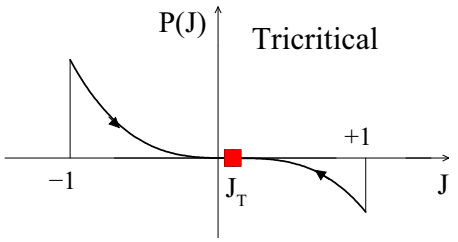

FIG. 4. (Color online) Tricritical dynamical behavior ($J_1 = J_2 = J_3 = J_T$).

C. Tricritical dynamics

When all three fixed points merge at some J_T, the dynamical system (13) exhibits a pitchfork bifurcation [54]. In physical terms, this corresponds to tricritical behavior. We have then

$$P(J_T) = P'(J_T) = P''(J_T) = 0, \tag{26}$$

so that the tricritical synaptic strength J_T is a triple zero of the rate function $P(J)$ (see Fig. 4).

The mean synaptic strength again exhibits a universal power-law relaxation (even slower than at the critical points) to its tricritical value J_T:

$$J(t) - J_T \approx \pm\frac{B_T}{\sqrt{t}}. \tag{27}$$

This $1/\sqrt{t}$ relaxation law holds irrespective of the initial value $J(0)$, with $\pm$ denoting the sign of the initial difference $J(0) - J_T$, whereas

$$B_T = \sqrt{-\frac{3}{P'''(J_T)}} = \frac{1}{\sqrt{8\delta\varepsilon^2 J_T}}. \tag{28}$$

As J_T is always positive, the expression on the right-hand side is always well defined. We have actually $J_T > \frac{1}{3}$ [see (36)], and so the tricritical point too is always strengthening.

To sum up, the noncritical fixed points of regimes I or II are characterized by exponential relaxation; the corresponding relaxation times, whether long or short, are always finite. Anywhere along the critical manifold, on the other hand, one observes a universal power-law relaxation in $1/t$ of the mean synaptic strength. An even slower power-law relaxation in $1/\sqrt{t}$ holds at the tricritical point. These two cases correspond to an infinite relaxation time.

IV. DEPENDENCE ON PARAMETERS AND PHASE DIAGRAM

We have so far described the various dynamical regimes characterizing the evolution of the mean synaptic strength $J(t)$ according to the mean-field dynamical equation (13). Here, we describe the regions of parameter space where these will be found.

A. Dependence on the spontaneous rates

It is worth examining first the phase diagram of the model in the ω-Ω plane of the spontaneous rates, for fixed values of ε, α, and δ. This plane is also the arena where input signals are expressed (see Sec. V).

The criticality conditions (23) allow us to express the critical values of the spontaneous rates in terms of J_c as

$$\omega_c = \tfrac{1}{2}\big(-3p_4J_c^4 + 4p_4J_c^3 - p_2J_c^2 + 2p_2J_c - \alpha - \delta\big),$$
$$\Omega_c = \tfrac{1}{2}\big(3p_4J_c^4 + 4p_4J_c^3 + p_2J_c^2 + 2p_2J_c - \alpha + \delta\big). \quad (29)$$

At the tricritical point, the third equality of (26) determines the value of J_T as:

$$J_T^2 = -\frac{p_2}{6p_4} = \frac{1}{6}\left(\frac{\alpha+\delta}{\delta} + \frac{1}{\varepsilon^2}\right). \quad (30)$$

From now on, J_T will denote the (positive) square root of this expression.

The expressions (29) of the critical rates imply

$$\frac{\partial\omega_c}{\partial J_c} = -6\delta\varepsilon^2(1-J_c)\big(J_c^2 - J_T^2\big),$$
$$\frac{\partial\Omega_c}{\partial J_c} = -6\delta\varepsilon^2(1+J_c)\big(J_c^2 - J_T^2\big). \quad (31)$$

Viewed as functions of J_c, both critical rates are therefore simultaneously stationary (i.e., either maximal or minimal) for $J_c = \pm J_T$. The only way for the model to have a physical tricritical point, where both spontaneous rates ω_T and Ω_T are positive, is to have $\delta > 0$, i.e., $\gamma > \beta$, and $J = J_T > 0$. The spontaneous rates are then maximal at this tricritical point.

Figure 5 shows a schematic phase diagram in the ω-Ω plane. The horn-shaped curve is the critical manifold ending in a cusp singularity at the tricritical point T. The upper branch (L) corresponds to left critical dynamics, while the lower one (R) corresponds to right critical dynamics. The bounded region inside the critical curve corresponds to regime II, while the complementary region corresponds to regime I.

B. Dependence on the other parameters

Let us now examine the phase diagram of the model as a function of the remaining parameters ε, α, and δ. The two latter rates only enter through their ratio, which suggests the definition of the dimensionless quantity

$$g = \frac{\delta}{\alpha+\delta}. \quad (32)$$

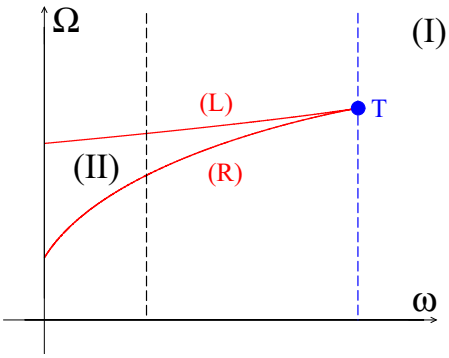

FIG. 5. (Color online) Schematic phase diagram in the ω-Ω plane. T: tricritical point. (L) and (R): left and right critical branches. (I) and (II): Regimes I and II. Vertical dashed lines: cuts along which fixed points and relaxation times will be investigated in Sec. IV C and plotted in Figs. 7 and 8.

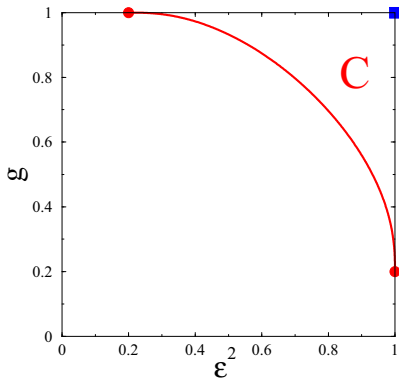

FIG. 6. (Color online) Phase diagram in the ε^2-g parameter space. The model has a physical critical manifold in the region marked with C. (Red) curve ending at filled circles: phase boundary [see (33)] with endpoints ($\varepsilon^2 = \frac{1}{5}$, $g = 1$) and ($\varepsilon^2 = 1$, $g = \frac{1}{5}$). (Blue) filled square: extremal model ($\varepsilon^2 = g = 1$).

The tricritical values Ω_T and ω_T of the spontaneous rates Ω and ω turn out to obey $\Omega_T > \omega_T$. The condition for having a physical critical manifold resembling Fig. 5, culminating in a physical tricritical point, is thus $\omega_T > 0$.

Figure 6 shows the phase diagram of the model in the ε^2-g parameter space (the unit square). The (red) curve with equation

$$128\varepsilon^2 g(\varepsilon^2+g)^3 = 3(\varepsilon^4 + 14\varepsilon^2 g + g^2)^2 \quad (33)$$

is the phase boundary, corresponding to $\omega_T = 0$. This curve exhibits an unexpected symmetry under the exchange of ε^2 and g. The endpoints, shown as red symbols, have coordinates ($\varepsilon^2 = \frac{1}{5}$, $g = 1$) and ($\varepsilon^2 = 1$, $g = \frac{1}{5}$).

The model exhibits critical behavior only when the parameters ε^2 and g lie above the red curve, i.e., in the rather small region marked C. These rather stringent limitations on critical behavior suggest that the associated infinitely large relaxation time is only rarely observed: most of the phase diagram is dominated by exponential relaxation. This is consistent with the fact that one would expect infinitely large relaxation times (with their possible association with long-term memory, see Sec. V) to be associated only with rare events.

The upper right corner of Fig. 6, shown as a (blue) square, corresponds to the extremal model where $\varepsilon^2 = 1$ (the slope of the response function is maximal) and $g = 1$, i.e., $\alpha = 0$ (absence of Hebbian learning). The tricritical synaptic strength assumes the value

$$J_T = \frac{1}{\sqrt{3}} \approx 0.57735. \quad (34)$$

In reduced time units where $\delta = 1$, the corresponding spontaneous rates read

$$\omega_T = \tfrac{2}{9}(2\sqrt{3} - 3) \approx 0.10313,$$
$$\Omega_T = \tfrac{2}{9}(2\sqrt{3} + 3) \approx 1.43646. \quad (35)$$

The critical manifold is the largest possible in this extremal model. With the notation of Fig. 5, the left (L) branch corresponds to $\frac{1}{3} < J_c^{(\mathrm{L})} < J_T$, while the right (R) branch corresponds to $J_T < J_c^{(\mathrm{R})} < 1$. It can be checked that the range

of possible values of J_c is always smaller for generic parameter values in region C of Fig. 6, than in this extremal model. In particular, we always have

$$J_c > \tfrac{1}{3}. \tag{36}$$

C. Relaxation times

In this section we illustrate the behavior of the attractive fixed points of the mean-field dynamical equation (13), and of the corresponding relaxation times. The main emphasis is on the divergent behavior of the relaxation times when the critical manifold or the tricritical point is approached. The subsequent numbers and figures correspond to the extremal model ($\varepsilon^2 = g = 1$). This choice is only made for convenience; any point within region C of Fig. 6 would lead to a similar picture. Finally, we work in reduced time units ($\delta = 1$).

1. Critical behavior

In order to investigate the effect of the critical manifold, we fix a value $\omega = 0.03$ and move along the left (black) vertical line of Fig. 5 by varying Ω. By so doing, we cross the left critical branch (L) at $\Omega_c^{(\mathrm{L})}$ and the right critical branch (R) at $\Omega_c^{(\mathrm{R})}$.

Figure 7 shows the fixed points (top) and the corresponding relaxation times (bottom) against the potentiating rate Ω. In regime II, i.e., for $\Omega_c^{(\mathrm{R})} < \Omega < \Omega_c^{(\mathrm{L})}$, the figure shows the two attractive fixed points, J_1 [lower (black) branch] and J_2 [upper (red) branch] and the two associated relaxation times, τ_1 and τ_2. The intermediate repulsive fixed point J_3 (blue) is also shown for completeness. One relaxation time diverges as each branch of the critical manifold is reached. As $\Omega \to \Omega_c^{(\mathrm{L})}$, where J_1 and J_3 merge at $J_c^{(\mathrm{L})}$ (see Fig. 3, top), we have

$$J_c^{(\mathrm{L})} - J_1 \sim \left(\Omega_c^{(\mathrm{L})} - \Omega\right)^{1/2}, \quad \tau_1 \sim \left(\Omega_c^{(\mathrm{L})} - \Omega\right)^{-1/2}. \tag{37}$$

Similarly, as $\Omega \to \Omega_c^{(\mathrm{R})}$, where J_2 and J_3 merge at $J_c^{(\mathrm{R})}$ (see Fig. 3, bottom), we have

$$J_2 - J_c^{(\mathrm{R})} \sim \left(\Omega - \Omega_c^{(\mathrm{R})}\right)^{1/2}, \quad \tau_2 \sim \left(\Omega - \Omega_c^{(\mathrm{R})}\right)^{-1/2}. \tag{38}$$

Outside the interval $\Omega_c^{(\mathrm{R})} \leqslant \Omega \leqslant \Omega_c^{(\mathrm{L})}$, we are in regime I. There is one single fixed point J_0 (see Fig. 2, top). This fixed point appears as a continuation of J_1 for $\Omega < \Omega_c^{(\mathrm{R})}$, and as a continuation of J_2 for $\Omega > \Omega_c^{(\mathrm{L})}$.

2. Tricritical behavior

Now, in order to investigate the effect of the tricritical point, we set $\omega = \omega_T$ [see (35)] and vary Ω, which traces the right (blue) vertical line of Fig. 5. Consequently, we are always in regime I, with its single fixed point J_0 and corresponding relaxation time τ_0. These quantities are plotted in Fig. 8. As the tricritical point is approached ($\Omega \to \Omega_T$), we have the power laws

$$|J_0 - J_T| \sim |\Omega - \Omega_T|^{1/3}, \quad \tau_0 \sim |\Omega - \Omega_T|^{-2/3}. \tag{39}$$

3. Summary

We now summarize the content of the above paragraphs. In the critical regime, the power laws (37), (38) are characteristic of a saddle-node bifurcation. They together conspire to hint at the slow relaxation in $1/t$ [see (24)] of the mean synaptic strength at a critical point. Similarly, in the tricritical regime, the relaxation in $1/\sqrt{t}$ [see (27)] at the tricritical point results from combining the power laws (39), which are characteristic of a pitchfork bifurcation. The first thing worth remarking is that the divergence of the tricritical relaxation time is symmetric when Ω_T is approached from smaller and larger Ω. This is not the case for the critical regime, when the divergence occurs at $\Omega_c^{(\mathrm{L})}$ when approached from below and at $\Omega_c^{(\mathrm{R})}$ when approached from above. Second, the faster growth of the relaxation time around the tricritical point causes the overall slower relaxation of the mean synaptic strength, with respect to the critical regime.

We end this section with a qualitative picture of our phase diagram and its associated flows. The choice of g and ε defines a specific model within the region C of Fig. 6. The behavior of the latter as a function of Ω and ω is illustrated in Fig. 5. Here, ω can be chosen such that, upon varying Ω, the system is:

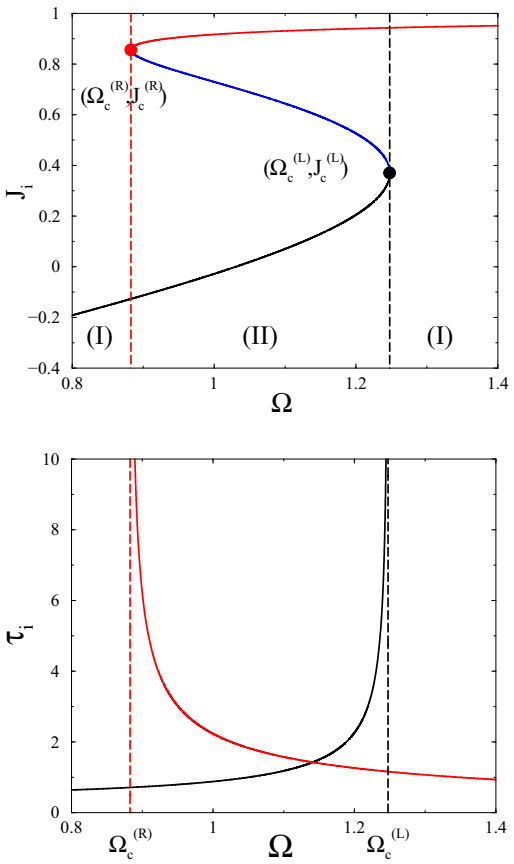

FIG. 7. (Color online) Top: Fixed points J_i against potentiating rate Ω in reduced units, for the extremal model with $\omega = 0.03$. Bottom (black) and top (red) curves: attractive fixed points. Intermediate (blue) curve: repulsive fixed point. Right (black) and left (red) filled symbols have respective coordinates ($\Omega_c^{(\mathrm{L})} \approx 1.24768$, $J_c^{(\mathrm{L})} \approx 0.37013$) and ($\Omega_c^{(\mathrm{R})} \approx 0.88270$, $J_c^{(\mathrm{R})} \approx 0.85650$). Bottom: relaxation times associated with the attractive fixed points. Vertical lines at $\Omega = \Omega_c^{(\mathrm{L})}$ and $\Omega = \Omega_c^{(\mathrm{R})}$ demarcate regimes I and II and locate the divergences (37), (38).

(i) fully confined to the noncritical regime I ($\omega > \omega_T$) so that only exponential relaxation is possible.

(ii) constrained to reach the tricritical point ($\omega = \omega_T$). Here, all initial configurations of synapses (ranging from totally weak to totally strong) are attracted towards a unique tricritical point, which is strengthening ($J_T > 0$). The consequent power-law relaxation ($\sim 1/\sqrt{t}$) is at its slowest here.

(iii) free to explore the critical region ($\omega < \omega_T$). For $\Omega < \Omega_c^{(\mathrm{R})}$ and $\Omega > \Omega_c^{(\mathrm{L})}$, the system is in regime I, and all relaxation is exponential. For $\Omega_c^{(\mathrm{R})} < \Omega < \Omega_c^{(\mathrm{L})}$, whether the critical point is reached or not depends strongly on the initial synaptic configuration through $J(0)$. While both fixed points are strengthening, the important difference with the tricritical scenario is that the associated power-law forgetting is faster ($\sim 1/t$) here.

The relaxation time for the mean synaptic strength is likely to provide an upper bound for the relaxation time of specific patterns stored in a distributed fashion across the network. Consequently, as will be discussed in the next section, the critical and tricritical situations are those where power-law forgetting can be manifested.

V. LEARNING AND FORGETTING

A. Global properties

In this section we address the learning and forgetting properties of the model network. We start with global features,

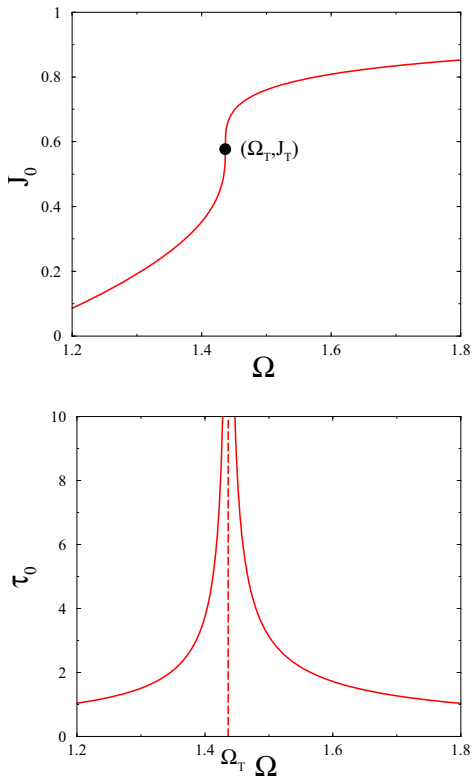

FIG. 8. (Color online) Top: attractive fixed point J_0 against potentiating rate Ω in reduced units, for the extremal model with $\omega = \omega_T$. The coordinates (Ω_T, J_T) of the tricritical point (filled symbol) are given by (34), (35). Bottom: associated relaxation time τ_0. The vertical line at $\Omega = \Omega_T$ locates the divergence (39).

by submitting our model to an arbitrary time-dependent but spatially uniform input. The latter is modeled by two deterministic signals $S(t)$ and $s(t)$, which are respectively superposed on the spontaneous relaxation rates, according to

$$\begin{aligned} \Omega(t) &= \Omega + S(t), \\ \omega(t) &= \omega + s(t). \end{aligned} \tag{40}$$

The single collective degree of freedom of the model, namely its mean synaptic strength $J(t)$, evolves according to Eq. (13), where the rate function

$$\begin{aligned} P(J;t) = {} & p_4 J^4 + p_2 J^2 \\ & - [\Omega + \omega + \alpha + S(t) + s(t)]J \\ & + \Omega - \omega - \delta + S(t) - s(t) \end{aligned} \tag{41}$$

now bears an explicit time dependence.

Let us assume for definiteness that the mean synaptic strength has relaxed to one of its fixed-point values J, and that the signals $S(t)$ and $s(t)$ are nonzero only in a finite time window of duration T. During the learning phase ($0 < t < T$), $J(t)$ will be displaced from the fixed-point value J, characterizing its default state in the absence of any input. During the subsequent forgetting phase ($t > T$), $J(t)$ will relax back to its default state.

If the default parameters are such that the system lies in the noncritical regime, then both learning and forgetting will be exponentially fast. Optimal trajectories can in principle be constructed, as was done in Refs. [43,44] so that fast learning and slow(er) forgetting are obtained, but globally, the memory manifested is always short-term. If, however, the default state of the model is critical, the application of generic input signals will take the system off it, so that the learning mechanism will be characterized by a finite relaxation time. Learning will thus be exponentially fast, while forgetting (at the same global level) will follow the power law (24) characteristic of the critical state.

B. Local properties

Associative memory is usually encoded in patterns, which are stored throughout neural networks in a distributed fashion, i.e., as a nonuniform modulation of the synaptic weights σ_{ij}. In order to explore the storage of memory in our model, an arbitrary space and time-dependent input [modeled as deterministic signals $S_{ij}(t)$ and $s_{ij}(t)$] would have to be superposed on the spontaneous relaxation rates of every synapse (ij):

$$\begin{aligned} \Omega_{ij}(t) &= \Omega + S_{ij}(t), \\ \omega_{ij}(t) &= \omega + s_{ij}(t). \end{aligned} \tag{42}$$

The resulting equations can only be investigated by means of extensive numerical work in the general case.

We can however look analytically at the response of a single synapse, say (kl), when it is submitted to an input such as (42). The mean synaptic strength $J(t)$ of the whole network will be unaffected by such a localized perturbation, and thus continue to obey (13). Let us again assume that the system has reached one of the fixed-point values J. The stochastic dynamics of the selected synapse (kl) can be shown, along the lines of the

derivation of (15), to be determined by the effective rates

$$\begin{aligned}\Omega_{\rm eff}(t) &= \Omega + \tfrac{1}{2}\alpha(1+\varepsilon^2 J^2) \\ &\quad + \tfrac{1}{4}\beta(1+J)(1-\varepsilon^2 J^2) + S_{kl}(t), \\ \omega_{\rm eff}(t) &= \omega + \tfrac{1}{2}\alpha(1-\varepsilon^2 J^2) \\ &\quad + \tfrac{1}{4}\gamma(1-J)(1-\varepsilon^2 J^2) + s_{kl}(t).\end{aligned} \tag{43}$$

The mean strength $j_{kl}(t)$ of the selected synapse therefore obeys

$$\frac{dj_{kl}}{dt} = \Omega_{\rm eff}(t)(1-j_{kl}) - \omega_{\rm eff}(t)(1+j_{kl}). \tag{44}$$

In the forgetting phase ($t > T$), the input signals vanish, so that the mean strength of the selected synapse relaxes to the fixed-point value J of the mean synaptic strength of the whole network. Interestingly, this relaxation is always exponential:

$$j_{kl}(t) - J \sim {\rm e}^{-t/\tau_{\rm loc}}. \tag{45}$$

The corresponding local relaxation time is such that its reciprocal is the sum of both rates (43) in the absence of a signal, i.e.,

$$\frac{1}{\tau_{\rm loc}} = \Omega + \omega + \alpha + \tfrac{1}{4}[\beta(1+J) + \gamma(1-J)](1-\varepsilon^2 J^2). \tag{46}$$

This relaxation time is likely to provide a lower bound for time scales associated with short-term memory.

C. A rich spectrum of time scales

As indicated above, networks learn by assimilating space- and time-dependent patterns. Realistic learning and forgetting protocols depend on the precise space and time dependence of applied signals, as well as, of course, the default parameters of the network. In the previous two subsections, we have shown that global time scales associated with the dynamics of the entire network can be either finite (exponential relaxation) or infinite (power-law relaxation), while the relaxation of a single synapse is always exponential. The global and local time scales provide estimates for the upper and lower bounds respectively for learning and forgetting in realistic situations, which can involve all possible time scales in between. This generation of such a rich dispersive spectrum of time scales from a simple model of a synaptic network has enabled us to unify the hitherto somewhat separate [36,37] domains of modeling long- and short-term memory.

We remark that the default parameters of the model correspond to the intrinsic properties of the network: given this, it is rather fitting that the critical manifold is rather small, and has to satisfy rather stringent conditions in order to exist. In other words: while exponential forgetting is generic, one needs to design networks rather carefully to get long-term memory storage.

VI. DISCUSSION

Memories can be short- or long-lasting. Our ability to store information depends as much on our intrinsic neural structure, as well as, typically, the significance of this information. One of the most important features of the model presented here is that it provides a natural framework for this separation of time scales in terms of the default (intrinsic) state of the system and the nature of applied signals. Short-term memories are forgotten exponentially fast, with a whole spectrum of time scales determining how fast the forgetting actually is. Power-law forgetting may hold for long-term memories corresponding to the default state of the system being on a critical manifold; there, the mean synaptic strength has a universal $1/t$ fall off, which gets even slower at the tricritical point, where it is turned into a $1/\sqrt{t}$ behavior. Since the existing model for long-term memory relies on possibly unrealistic auxiliary structures such as internal states [36,37], our model represents an important conceptual advance in the field; it unifies the modeling of short- and long-term memory, which emerge naturally from collective synaptic dynamics, without the need to invoke special architectures.

This framework is also an appropriate one to discuss optimal learning. This occurs if the default state of a neural system lies on the critical manifold, so that fast learning will occur for generic signals (which will typically perturb the system to one of regimes I or II), while forgetting will be extremely slow. The dynamics in regime II may exhibit yet other phenomena, with the possibility of the degradation or improvement of the same system as a result of strong enough applied signals. The application of more complex protocols, i.e., time-dependent signals, on the present model would reveal a very rich dynamical behavior with a whole panoply of possible scenarios. As a rather extreme situation, one may think of complex learning protocols, corresponding to signals cycling around the critical manifold or the tricritical point in the ω-Ω plane, and of the corresponding very unusual aging behavior.

We now make a few remarks on the design of our model. The slow plasticity dynamics of synapses are driven by competitive and cooperative interactions consequent on the fast dynamics of firing neurons. The model is analyzed within a mean-field approximation, in common with many physics-based approaches to neuroscience, ranging from earlier work [11–20] to more recent developments [55]. Such a mean-field framework is of course appropriate given the lack of knowledge of microscopic details at the neural or synaptic level. Our model includes some ideas presented in earlier work [43] but improves on them by cleanly separating the roles of neurons and synapses, as well as by introducing directedness. At the microscopic level, the introduction of directedness is quite complex, since for example, causality demands that synaptic updating occurs when a spike train from a presynaptic neuron reaches a postsynaptic neuron; this could lead to rather complicated rules reflecting such instantaneous, spike-time-dependent updates [47]. At our level of description involving much longer time scales, however, such spikes are averaged over and represented by a mean neural activity, which determines synaptic updates.

We should also add that the construction of alternative synaptic update rules to incorporate some aspects of this microscopic causality would, at least in the mean-field perspective presented here, not make much difference. In particular, introducing a nonlinear constitutive function $g(J)$ would only result in more intricate equations without changing any essential feature. In other words, the critical phenomena

exhibited by our model, and the global features of its phase diagram, are robust to microscopic details. The latter would of course regain their importance if our model were to be investigated by means of computer simulations on large networks.

Also, we point out that the cooperative Hebbian mechanism turns out to be almost entirely irrelevant to obtaining critical behavior in our model. On the other hand, a strong enough synaptic competitivity—the most original and important feature of this work—turns out to be the crucial ingredient for the potential manifestation of both short- and long-term memory in our model network. Since the human brain is thought of as being a vast and complex synaptic network, which also has this remarkable ability to store memories across a rich spectrum of time scales, our work underlines the current view that mechanisms of synaptic competitivity are of critical importance in neuroscience [5].

Finally, we make a few remarks on possible experiments to test our model. There has been a great deal of research into the idea that sleep consolidates short-term memories into long-term ones [56–58]; experiments on rats suggest that this transformation occurs via a hippocampus-cortical memory transfer [59]. In the context of our model, this would suggest that competitive mechanisms predominate in the cortex rather than the hippocampus; this idea provides a testable prediction for experiments *in vivo*. A possible *in vitro* experiment could involve the adaptation of high-resolution measurements of cultured cortical slices [60], which have been very successful in probing neuronal avalanches, to the present situation: since these methods are able to distinguish clearly between exponential and power-law signatures in neuronal avalanches, one might reasonably hope that they would be able to do the same in the context of stored synaptic memories.

ACKNOWLEDGMENTS

A.M. warmly acknowledges the hospitality of the Institut de Physique Théorique, where most of this work was conceived and carried out. She also thanks Konstantin Klemm for useful discussions on models of directed synapses.

[1] H. Ebbinghaus, *Memory: A Contribution to Experimental Psychology*, translated by H. A. Ruger and C. E. Bussenius (Dover, New York, 1964).
[2] L. R. Squire, Neurobiol. Learning and Memory **82**, 171 (2004).
[3] M. C. W. van Rossum and M. Shippi, J. Stat. Mech. (2013) P03007.
[4] G. G. Turrigiano and S. B. Nelson, Nature Reviews Neurosci. **5**, 97 (2004).
[5] A. van Ooyen, Nature Reviews Neurosci. **12**, 311 (2011).
[6] D. J. Amit, *Modeling Brain Function: The World of Attractor Neural Networks* (Cambridge University Press, Cambridge, 1999).
[7] P. Dayan and L. F. Abbott, *Theoretical Neuroscience: Computational and Mathematical Modeling of Neural Systems* (MIT Press, Cambridge, USA, 2001).
[8] W. Gerstner and W. M. Kistler, *Spiking Neuron Models: Single Neurons, Populations, Plasticity* (Cambridge University Press, Cambridge, 2002).
[9] J. J. Hopfield, Proc. Natl. Acad. Sci. USA **79**, 2554 (1982).
[10] J. J. Hopfield, Proc. Natl. Acad. Sci. USA **81**, 3088 (1984).
[11] D. J. Amit, H. Gutfreund, and H. Sompolinsky, Phys. Rev. Lett. **55**, 1530 (1985).
[12] D. J. Amit, H. Gutfreund, and H. Sompolinsky, Phys. Rev. A **32**, 1007 (1985).
[13] D. J. Amit, H. Gutfreund, and H. Sompolinsky, Phys. Rev. A **35**, 2293 (1987).
[14] D. J. Amit, H. Gutfreund, and H. Sompolinsky, Ann. Phys. (N.Y.) **173**, 30 (1987).
[15] J. P. Nadal, G. Toulouse, J. P. Changeux, and S. Dehaene, Europhys. Lett. **1**, 535 (1986).
[16] G. Parisi, J. Phys. A **19**, L617 (1986).
[17] D. J. Amit and S. Fusi, Network **3**, 443 (1992).
[18] D. J. Amit and S. Fusi, Neural Comput. **6**, 957 (1994).
[19] D. J. Amit and N. Brunel, Network **8**, 373 (1997).
[20] S. Romani, D. J. Amit, and Y. Amit, Neural Comput. **20**, 1928 (2008).
[21] N. Brunel and V. Hakim, Neural Comput. **11**, 1621 (1999).
[22] J. M. Beggs and D. Plenz, J. Neurosci. **23**, 11167 (2003).
[23] S. Bornholdt and T. Röhl, Phys. Rev. E **67**, 066118 (2003).
[24] A. Roxin, H. Riecke, and S. A. Solla, Phys. Rev. Lett. **92**, 198101 (2004).
[25] L. de Arcangelis, C. Perrone-Capano, and H. J. Herrmann, Phys. Rev. Lett. **96**, 028107 (2006).
[26] L. de Arcangelis and H. J. Herrmann, Proc. Natl. Acad. Sci. USA **107**, 3977 (2010).
[27] A. Levina, J. M. Herrmann, and T. Geisel, Nature Phys. **3**, 857 (2007).
[28] A. Levina, J. M. Herrmann, and T. Geisel, Phys. Rev. Lett. **102**, 118110 (2009).
[29] M. Uhlig, A. Levina, T. Geisel, and J. M. Herrmann, Frontiers Comput. Neurosci. **7**, 87 (2013).
[30] T. J. Taylor, C. Hartley, P. L. Simon, I. Z. Kiss, and L. Berthouze, J. Math. Neurosci. **3**, 5 (2013).
[31] P. Bak, *How Nature Works: The Science of Self-Organized Criticality* (Springer, New York, 1996).
[32] M. I. Rabinovich, P. Varona, A. I. Selverston, and H. D. I. Abarbanel, Rev. Mod. Phys. **78**, 1213 (2006).
[33] J. T. Wixted and E. B. Ebbesen, Psychol. Sci. **2**, 409 (1991).
[34] J. T. Wixted and E. B. Ebbesen, Mem. Cognit. **25**, 731 (1997).
[35] C. T. Kello, G. D. A. Brown, R. Ferrer-I-Cancho, J. G. Holden, K. Linkenkaer-Hansen, T. Rhodes, and G. C. van Orden, Trends Cogn. Sci. **14**, 223 (2010).
[36] S. Fusi, P. J. Drew, and L. F. Abbott, Neuron **45**, 599 (2005).
[37] A. Mehta and J. M. Luck, J. Stat. Mech. (2011) P09025.
[38] A. Mehta, J. M. Luck, C. C. Luk, and N. I. Syed, PLoS ONE **8**, e78056 (2013).
[39] A. B. Barrett, G. O. Billings, R. G. M. Morris, and M. C. W. van Rossum, PLoS Comput. Biol. **5**, e1000259 (2009).

[40] D. O. Hebb, *The Organization of Behavior: A Neuropsychological Theory* (Wiley, New York, 1949).
[41] C. Castellano, S. Fortunato, and V. Loreto, Rev. Mod. Phys. **81**, 591 (2009).
[42] A. Mehta and J. M. Luck, Phys. Rev. E **60**, 5218 (1999).
[43] G. Mahajan and A. Mehta, Europhys. Lett. **95**, 48808 (2011).
[44] A. A. Bhat, G. Mahajan, and A. Mehta, PLoS ONE **6**, e25048 (2011).
[45] K. D. Miller, Neuron **17**, 371 (1996).
[46] G. G. Turrigiano, K. R. Leslie, N. S. Desai, L. C. Rutherford, and S. B. Nelson, Nature (London) **391**, 892 (1998).
[47] S. Song, K. D. Miller, and L. Abbott, Nature Neurosci. **3**, 919 (2000).
[48] P. J. Sjöström, G. G. Turrigiano, and S. B. Nelson, Neuron **32**, 1149 (2001).
[49] S. Song, P. J. Sjöström, M. Reigl, S. Nelson, and D. B. Chklovskii, PLoS Biol. **3**, e68 (2005).
[50] C. van Vreeswijk and H. Sompolinsky, Science **274**, 1724 (1996).
[51] C. van Vreeswijk and H. Sompolinsky, Neural Comput. **10**, 1321 (1998).
[52] M. Benayoun, J. D. Cowan, W. van Drongelen, and E. Wallace, PLoS Comput. Biol. **6**, e1000846 (2010).
[53] N. G. van Kampen, *Stochastic Processes in Physics and Chemistry* (North-Holland, Amsterdam, 1992).
[54] S. H. Strogatz, *Nonlinear Dynamics and Chaos, With Applications to Physics, Biology, Chemistry and Engineering* (Perseus, Reading, Massachusetts, 1994).
[55] M. Breakspear, J. A. Roberts, J. R. Terry, S. Rodrigues, N. Mahant, and P. A. Robinson, Cereb. Cortex **16**, 1296 (2006).
[56] S. Diekelmann and J. Born, Nature Reviews Neurosci. **11**, 114 (2010).
[57] S. Chauvette, J. Seigneur, and I. Timofeev, Neuron **75**, 1105 (2012).
[58] G. Yang, C. S. W. Lai, J. Cichon, L. Ma, W. Li, and W. B. Gan, Science **344**, 1173 (2014).
[59] S. Ribeiro, X. Shi, M. Engelhard, Y. Zhou, H. Zhang, D. Gervasoni, S. C. Lin, K. Wada, N. A. M. Lemos, and M. A. L. Nicolelis, Frontiers Neurosci. **1**, 43 (2007).
[60] N. Friedman, S. Ito, B. A. W. Brinkman, M. Shimono, R. E. Lee DeVille, K. A. Dahmen, J. M. Beggs, and T. C. Butler, Phys. Rev. Lett. **108**, 208102 (2012).